International Conference on Control, Engineering & Information Technology (CEIT'14)
Proceedings - Copyright IPCO-2014
ISSN 2356-5608

A Static Var Compensator Controlled Topology Based on TCR-TSC for a Grid Connected Photovoltaic System

Salwa Akermi[1] *, Noureddine Hidouri*[2] *, Lassâad Sbita*[3]

[1]akremi.salwa@gmail.com, [2]noureddine.hidouri@yahoo.fr, [3]lassaad.sbita@enig.rnu.tn

Research Unit of Photovoltaic, Wind turbine and Geothermal Systems
National Engineering School of Gabes, Tunisia

***Abstract*— This paper illustrates the use of Static Var Compensators (SVC) to control the performance of a grid connected photovoltaic system (GCPS). The compensator considered in this work contains one Thyristor Controlled Reactor (TCR) and three Thyristors Switched Capacitors (TSC), which are two of the shunt Flexible Altering Current Transmission Systems (FACTS) devices. The proposed configuration incorporates a photovoltaic array, a boost converter, an inverter that generates a three phase supply that will be filtered and connected to the grid through a step up transformer and a non linear load. The positive effect of the TCR and TSC-based SVC on the non linear load current is confirmed by the simulations results.**

Keywords*— *GCPS, TCR, TSC, Nonlinear load, SVC.

I. INTRODUCTION

The use of renewable energy such as photovoltaic is the subject of countless studies, since this kind of sources is nature, renewable and environmentally friend. The Grid Connected Photovoltaic System is one of the many applications of photovoltaic areas [1], [2], [5].

When connecting a PV system to the grid many undesirable impacts may occur such as rapid changes in power, current harmonics that can cause the pollution of the grid, including the instability of the grid system. To solve those problems Flexible Alternating Current Transmission Systems (FACTS) can be developed.

FACTS devices have been increasingly used in many electrical power systems, this technology based on electronic power devices, can improve the performance of power system by controlling the active and reactive power flow and increasing the stability of the system [6], [7], [11]. The FACT Systems can also eliminate current harmonics that can be injected into the power system.

The SVC (Static Var Compensator) is a parallel compensator of FACTS family; it can regulate the voltage in the power system by generating or absorbing reactive power from the system. The reactive power controlled by the SVC can be either capacitive or inductive depending whether the SVC generates or absorbs reactive power [8], [9].

There are many types of SVC controller, the Thyristor Switched Capacitor (TSC), which can perform the variation of reactive power by switching on and off a shunt capacitors banks using two anti-parallel thyristors [9], [11] and the Thyristor Controlled Reactor (TCR) which is a shunt reactors banks that can be switched on and off by two anti-parallel thyristors to control the variation of reactive power in the system [16].

In many cases we can combine the TCR and the TSC; this configuration can increase the stability of the system, ensured a continuous control of the reactive power, and eliminate the harmonics components [16].

In this paper we will present a technique for controlling the grid connected photovoltaic system using the SVC controller, principally three TSCs and one TRC as shown in fig.1

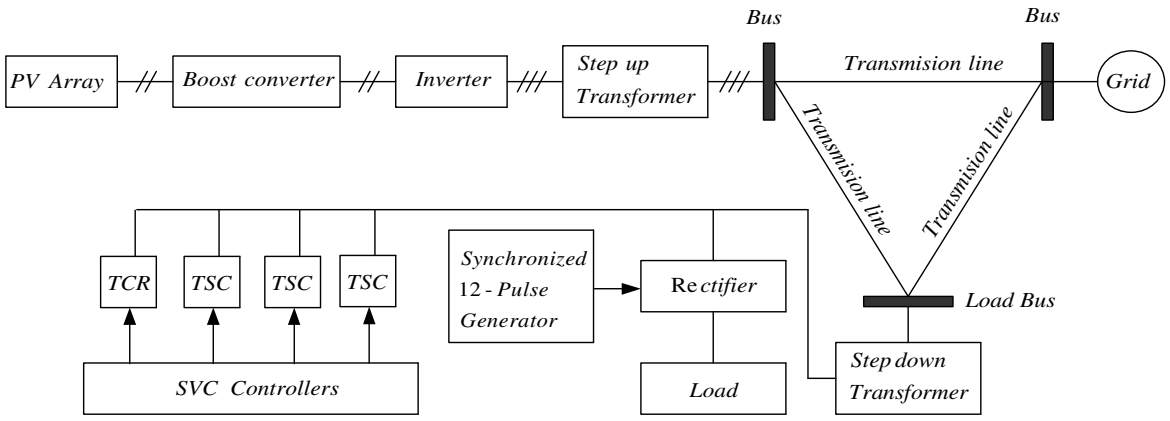

Fig.1. Proposed topology of the grid connected photovoltaic system.

II. THE GRID CONNECTED SYSTEM MODEL

A. *Modeling of the cell and PV array*

The solar cell is an electric device that can convert the solar energy into electrical one. In the literature many models are proposed for solar cells [3-5].

The electric equivalent circuit proposed in this work is shown in fig.2 [12-14]

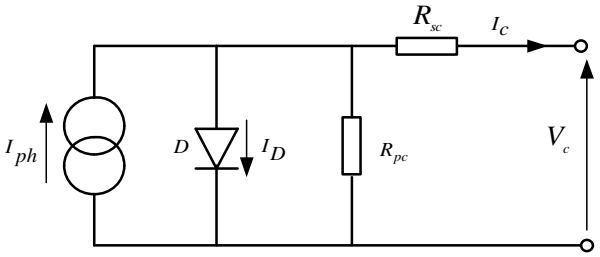

Fig. 2. Equivalent solar cell's electric circuit.

The characteristic equation of the cell's current I_c and cell's voltage V_c is represented by equation (1).

$$I_c = I_{ph} - I_{rs}\left(\exp\left(\frac{q}{\beta k T_c}\left(V_c + R_{sc} I_c\right)\right) - 1\right) - \frac{\left(V_c + R_{sc} I_c\right)}{R_{pc}} \quad (1)$$

Where I_{ph} is the photocurrent cell given by relation (2)

$$I_{ph} = \frac{G}{G_{ref}}\left(I_{sc\_ref} + K_{SCT}\left(T_c - T_{c\_ref}\right)\right) \quad (2)$$

Denote by G, T_c, K_{SCT} respectively the solar irradiation, the cell junction temperature and the short circuit current temperature coefficient. The photocurrent I_{ph_ref} is equal to the reverse saturation current I_{sc_ref} at the reference condition defined by T_{c_ref} and G_{ref} [4], [14].

I_{rs} is the reverse saturation current given by relation (3), where E_g, q, k and β are respectively the band gap energy of the semiconductor, the electron charge, the ideal factor of the solar cell and the βoltzman constant.

$$I_{rs} = I_{rs\_ref}\left(\frac{T_c}{T_{c\_ref}}\right)\exp\left[\frac{qE_g}{\beta k}\left(\frac{1}{T_c} - \frac{1}{T_{c\_ref}}\right)\right] \quad (3)$$

A module PV can contain n_s cells associated in series, a solar panel is composed of N_p array of modules associated in parallel; each array can be composed of N_s modules assembled in series. According to this consideration, we can express the relations between the panel's and the cells parameters in relation (4).

$$\begin{cases} I_p = N_p I_c \\ V_p = n_s N_s V_c \\ R_{sp} = \dfrac{n_s N_s}{N_p} R_{sc} \\ R_{pp} = \dfrac{n_s N_s}{N_p} R_{pc} \end{cases} \quad (4)$$

In this consideration, the equation related the panel current I_p to its voltage V_p is given in (5).

$$I_p = N_p I_{ph} - N_p I_{rs}\left(\exp\frac{q}{\beta k T_c}\left(\frac{V_p}{n_s N_s} + \frac{R_{sc} I_P}{N_p}\right) - 1\right) - \frac{N_p}{R_{pc}}\left(\frac{V_p}{n_s N_s} + \frac{R_{sc} I_P}{N_p}\right) \quad (5)$$

B. *Model of the Boost converter*

Fig.3, show the structure of the boost converter connected to the photovoltaic system and used in this work [13].

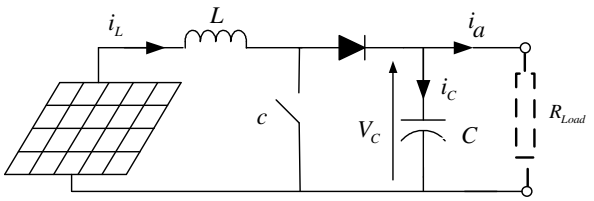

Fig. 3. Schematic of the boost converter

We suppose that the power devices in this model are ideal.

The command of the boost converter depends on the state of the switch that is controlled by a PWM signal characterized by the duty cycle (α) and the operating period (T), so during the operating time period (T), the switch is closed in αT, so c takes value (c=1) and the diode is switched off. In (1-α)T, the switch is open, c takes value (c=0) and the diode is switched on. According to this idea, the global model of the boost converter is given as:

$$\begin{bmatrix} \dot{i}_L \\ \dot{V}_C \end{bmatrix} = \begin{bmatrix} -\frac{R_L}{L} & -\frac{\bar{c}}{L} \\ \frac{\bar{c}}{C} & -\frac{1}{R_{Load}C} \end{bmatrix} \begin{bmatrix} i_L \\ V_C \end{bmatrix} + \begin{bmatrix} \frac{1}{L} \\ 0 \end{bmatrix} V_{panel} \tag{6}$$

$$V_{dc} = [0 \quad 1][i_L \quad V_C]' \tag{7}$$

C. Modeling of the three phase voltage inverter

Fig.4 gives the general diagram of a three-phase voltage inverter used in this work. [12], [15].

The Switches of each arm are complementary and it is the same for the associated command signals. [12], [15] so:

$$\begin{cases} c_4 = 1 - c_1 \\ c_5 = 1 - c_2 \\ c_6 = 1 - c_3 \end{cases} \tag{8}$$

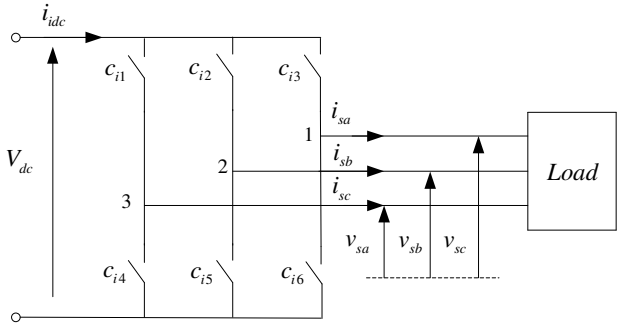

Fig. 4. Inverter-Load Configuration.

When the natural frame is used, the three output inverter voltage can be expressed by the relation (9)

$$\begin{bmatrix} v_{sa} \\ v_{sb} \\ v_{sc} \end{bmatrix} = \frac{V_{dc}}{3} \begin{bmatrix} -2 & 1 & 1 \\ 1 & -2 & 1 \\ 1 & 1 & -2 \end{bmatrix} \begin{bmatrix} c_{i4} \\ c_{i5} \\ c_{i6} \end{bmatrix} \tag{9}$$

In a fixed Concordia frame reference the output inverter voltage is given by (10), the following relation is built all around $(c_4, c_5 \text{ and } c_6)$ as Boolean variables defining the states of the inverter lower keys and the input DC voltage, [12], [15].

$$\bar{v} = v_d + jv_q = \sqrt{\frac{2}{3}} V_{dc} \left(c_4 e^{j\pi} + c_5 e^{j\frac{5\pi}{3}} + c_6 e^{j\frac{\pi}{3}} \right) \tag{10}$$

According to relation (10), the inverter voltage vectors expression are given by (11), [12], [15].

$$\begin{cases} \bar{v}_{sk} = 0 & if \quad k = 0 \ or \ \ k = 7 \\ \begin{cases} \bar{v}_{sk} = q^{(k-1)} \bar{v}_{s1} \\ \bar{v}_{s1} = \sqrt{\frac{2}{3}} V_{dc} \end{cases} & if \quad k = 1, 2, ...6 \\ q = e^{j\frac{\pi}{3}} \end{cases} \tag{11}$$

the inverter vectors expression are supported by 8 vectors that can be classified in two groups; the first one is composed of two null vectors, the second is composed of 6 vectors that can be presented as a geometric progression defined by the first term $\sqrt{\frac{2}{3}} V_{dc}$ and the ratio $e^{j\frac{\pi}{3}}$. Taking those into considerations, the active vectors form a balanced voltage system; having the same module and a regular phases. The space representation of these is illustrated by fig.5.

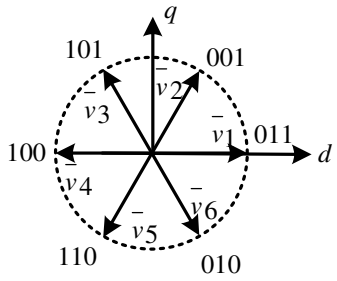

Fig. 5. Diagram of the three-phase inverter voltage vectors.

D. Modeling of the Thyristor Switched Capacitor (TSC)

Fig.6 shows the single phase structure of the Thyristor Switched Capacitor (TSC). The TSC consists of two anti-parallel thyristors in series with a capacitor that will be switched on or off, a small series resistance and inductance [10], [11].

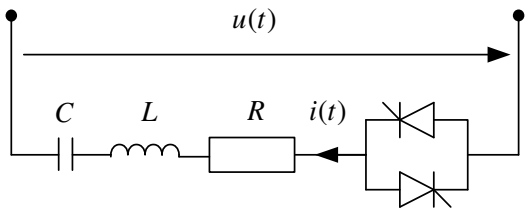

Fig. 6. Main structure of TSC.

The mathematic equations of the circuit when the series resistance is ignored are given as follow:

$$u = U_m \sin(\omega t + \varphi) = L\frac{di}{dt} + \frac{1}{C}\int i dt \tag{12}$$

$$\frac{d^2 i}{dt^2} + \frac{i}{LC} = \frac{U_m}{L}\cos(\omega t + \varphi) \tag{13}$$

The inductance initial current and the capacitance initial voltage are given by (14)

$$\begin{cases} i(0^+) = i(0^-) = 0 \\ u(0^+) = u(0^-) = u_{co} \end{cases} \tag{14}$$

Using those conditions the solution of relation (13) is given by(15)

$$i = I_m \cos(\omega t + \varphi) - I_m \cos(\varphi)\cos(\omega_o t) - u_{co}\omega_o C \sin(\omega_o t) + \frac{U_m \omega_o C \sin(\varphi)}{1 - \omega^2 LC}\sin(\omega_o t) \tag{15}$$

Where $\left(\omega_o = \frac{1}{\sqrt{LC}}\right)$ is the oscillation frequency and I_m is the peak current

The current (15) reaches directly into stable state when the conditions given by (16) are satisfied, thus the current of this circuit can be expressed as (17).

$$\begin{cases} u_{co} = \pm\frac{U_m}{1 - \omega^2 LC} \\ \varphi = \pm\frac{\pi}{2} \end{cases} \tag{16}$$

$$i \simeq I_m \cos(\omega t + \frac{\pi}{2}) \tag{17}$$

E. Thyristor Controlled Reactor Model

A basic single-phase TCR comprises two anti-parallel thyristor connected in series with a reactor, as illustrated in Fig.7 [17]. The TCR is able to control the undesirable impacts of the load and reduce them

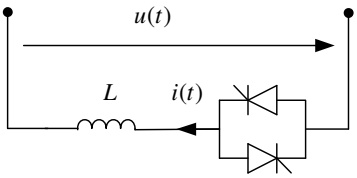

Fig. 7. TCR configuration

Using the structure given in fig.7, the mathematic relations are given by the following equations:

$$u = U_m \sin(\omega t) = L\frac{di}{dt} \tag{18}$$

Integrating (18), we get relation (19)

$$i(t) = \frac{1}{L}\int u(t) dt \tag{19}$$

$$i = -\frac{U_m}{\omega L}\cos(\omega t) + C \tag{20}$$

Where C is a constant

Using the initial condition given by (21), the solution of (19) is given by relation (22)

$$i(\alpha) = 0 \tag{21}$$

$$i = \frac{U_m}{\omega L}\left(\cos(\omega t) - \cos(\alpha)\right) \tag{22}$$

Where α is the TCR firing angle at which the thyristors are turned on and conduct a full half-period $90<\alpha<180$.

III. SIMULATION RESULTS

The simulation in this work has been carried out in Matlab/Simulink environment.

Fig. 8 and fig.9 give respectively the output panel and the output boost converter voltages

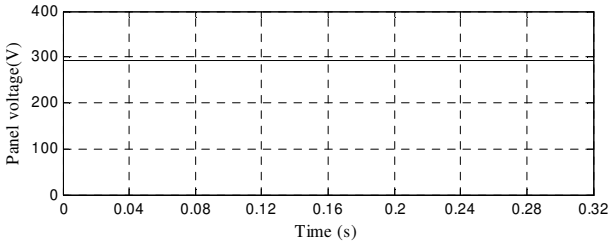

Fig. 8. Panel voltage response.

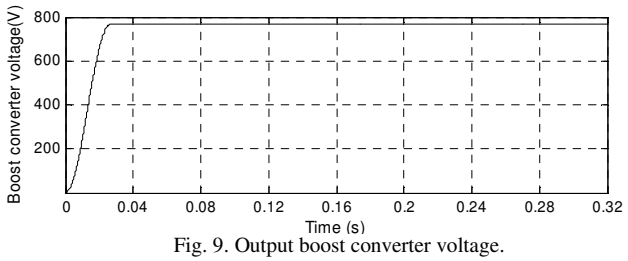

Fig. 9. Output boost converter voltage.

The output boost voltage is used as an input of the PWM controlled inverter. Fig.10, gives the response of the three phase voltage inverter.

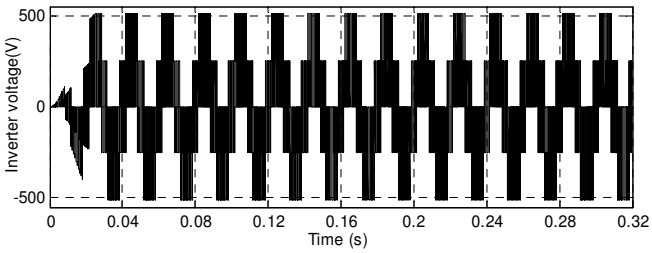

Fig. 10. Output inverter voltage.

The three phase voltages generated by the inverter shown in fig.10 are filtered using a filter grid, and then a step up transformer was used to adapt those voltages to the grid as shown in fig.1.

The filtered inverter voltage generated to the grid is shown in fig.11.

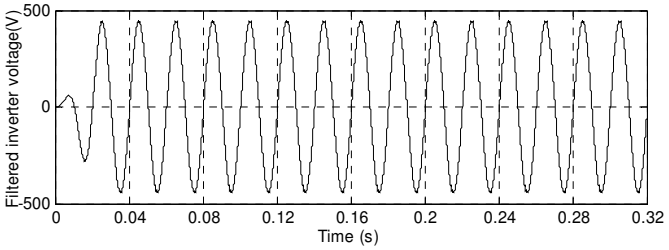

Fig. 11. Inverter voltage response.

In order to prove the influence the SVC, we have considered three cases;

***1- First case*:** at $t = 0.08\,s$ a nonlinear load is connected to the grid and the TCR-TSCs is not used. Fig.12 gives the wave of the DC Bus load current.

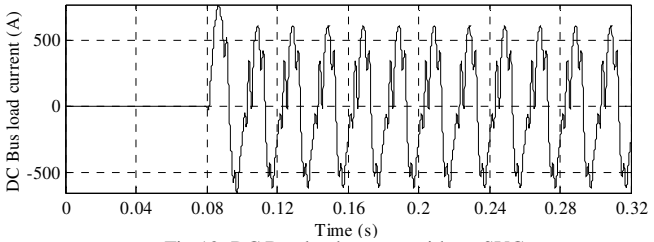

Fig.12. DC Bus load current without SVC.

As shown in fig.12, the wave shape of the current is affected by the harmonic phenomena caused by the nonlinear load, the harmonic spectrum and the THD value are given in fig.13

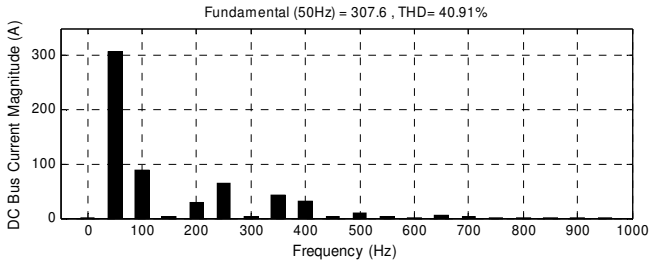

Fig.13. Harmonic spectrum of the DC Bus load current without SVC.

2- Second case: only the TSCs are connected to DC Bus load at $t = 0.16\,s$ .Fig. 14 shows that the wave of current is recovered by the use of the TSCs and the harmonic components have been almost eliminated.

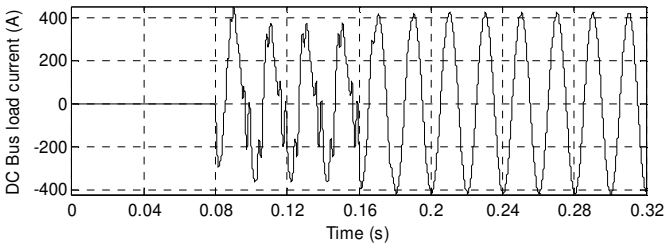

Fig. 14. DC Bus load current with TSCs.

The FFT analysis of fig.14 at t=0.16s, leads to fig.15 which represent the harmonic spectrum and the THD of the studied current with only TSCs. Compared to fig.13, this figure shows that the transient component of the load current is eliminated.

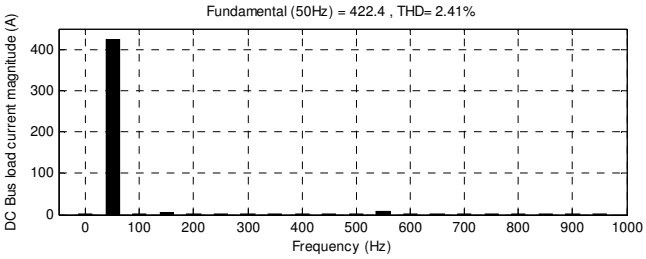

Fig. 15. Harmonic spectrum and THD of the DC bus load current using only three TSCs.

3-Third case: at t=0.24s a TCR is connected in parallel with the three TSCs to DC Bus load to show the performance of the whole compensator in harmonic elimination. Fig.16 and fig.17 gives respectively the wave of the DC Bus load current with both TCR and TSCs and the FFT analysis of the studied current

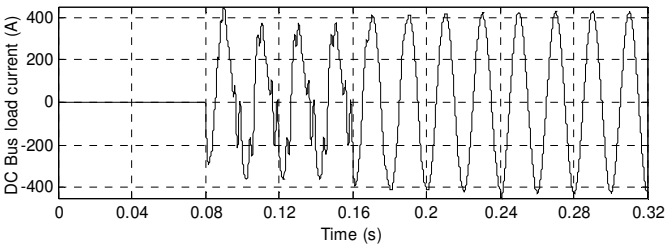

Fig. 16. DC Bus load current with TCR-TSCs

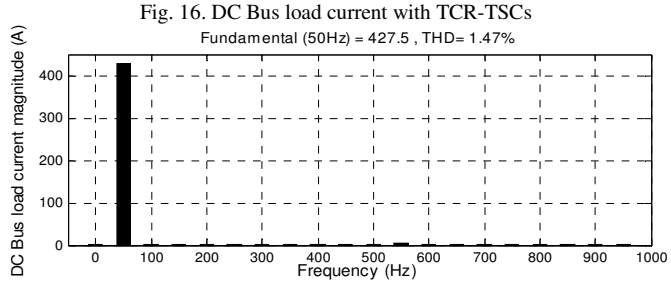

Fig. 17. Harmonic spectrum and THD of the DC bus load current using TCR-TSCs.

Compared the spectrum in fig.17 with those in fig.15 and fig.13, this spectrum show that the transient components of the load current are eliminated, and the result obtained by combining the TCR and the TSCs is better than using only

TSCs. The THD has decreased from 40.91% to 2.41% by using TSCs, while it reaches 1.47% with both TCR and TSCs.

IV. CONCLUSION

This paper introduces a controlled topology for a grid connected photovoltaic system based on SVC devices. Two most widely SVC devices TCR and TSC are used, modeled, and simulated in this paper. The simulation has been developed in Matlab/Simulink environment.

The case studied illustrate the impact of SVC devices principally the TCR-TSCs devices on a non linear load and the simulation results demonstrate that those devices can significantly eliminate the undesirable components generated by the load and injected into the system, which mean reduce the Total Harmonic Distortion. With the three TSCs the THD has been reduced from 40.91% to 2.41%, and it reaches to 1.41% when using the TCR with the three TSCs.

Appendix

TABLE I. GRID PARAMETERS

Source voltage	500KV
System frequency	50 Hz
Line R	26.07 Ω
Line L	48.86H

TABLE II. PARAMETERS OF TSC

Capacitance of TSC	308.4e-6 F
Inductance	1.13e-3 H
Resistance	4.26e-3 Ω

TABLE III. PARAMETERS OF TCR

Inductance	18.7e-9 H

TABLE IV. PARAMETERS OF CELL PV

Open circuit voltage Voc	0.6058 V
Short circuit current Isc	8.1 A
Parallel cell's resistance Rpc	0.833 Ω
Series cell's resistance Rsc	0.0833 mΩ
Solar cell's ideal factor k	1.450
Reverse diode saturation current Irs	3.047e-7 A
Short circuit current temperature coefficient KSCT	1.73e-3A/°K
Reference cell's temperature Tc_ref	25°C
Boltzman's constant β	1.38 e-23
Band gap energy Eg	1.11 ev

TABLE V. PARAMETERS OF PV MODULE

Rated output power	216W
Open circuit voltage: V_{oc}	36.35 V
Number of series cells: n_s	60

TABLE VI. PV ARRAY PARAMETERS

Open circuit voltage: V_{oc}	290 V
Short circuit current : I_{sc}	8.1 A
Number of series modules: N_s	8
Number of parallel modules: N_p	8

REFERENCES

[1] M. A. Mahmud, H. R. Pota, and M. J. Hossain, "Dynamic Stability of Three-Phase Grid-Connected Photovoltaic System Using Zero Dynamic Design Approach," IEEE Journal of Photovoltaics, Vol. 2(4), pp. 564-571, October 2012.

[2] K. Barra and D. Rahem, "Predictive direct power control for photovoltaic grid connected system: An approach based on multilevel converters," Energy Conversion and Management, 2013.

[3] K. H. Chao, S. H. Ho and M. H. Wang, "Modeling and fault diagnosis of a photovoltaic system," Electric Power Systems Research, vol. 78, pp. 97–105, 2008.

[4] R. Chenni, M. Makhlouf, T. Kerbache, and A. Bouzid, "A detailed modeling method for photovoltaic cells," Energy, vol. 32, pp. 1724–1730, 2007.

[5] L. S .Kim, "Sliding mode controller for the single phase grid connected photovoltaic system," Applied Energy, vol. 83, pp. 1101–1115, 2006.

[6] C. Rakpenthai, S. Premrudeepreechacharn and S. Uatrongjit, "Power system with multi-type FACTS devices states estimation based on predictor–corrector interior point algorithm," Electrical Power and Energy Systems, vol. 31, pp. 160–166, 2009.

[7] A.D. Del Rosso, C.A. Cañizares and V.M. Dona, "A Study of TCSC controller Design for Power Stability Improvement," IEEE transactions on power systems. Vol. 18, pp. 1487-1496, Nov. 2003.

[8] Ghorbani, M. Khederzadeh, and B.Mozafari, "Impact of SVC on the protection of transmission lines," Electrical Power and Energy Systems, vol. 42, pp. 702–709, 2012.

[9] S. K.M. Kodsi, C. A. Canizares , M. Kazerani, "Reactive current control through SVC for load power factor correction,". Electric Power Systems Research, vol. 76, pp. 701–708, 2006.

[10] A. Gelen and T. Yalcinoz, "An educational software package for Thyristor Switched Reactive Power Compensators using Matlab/Simulink," Simulation Modelling Practice and Theory, vol. 18, pp. 366–377, 2010.

[11] S. Akremi, N. Hidouri and L. Sbita, "A Static Var Compensator Controlled Topology For a Grid Connected Photovoltaic System," accepted in The International Renewable Energy Congress (IREC), March 25-27, 2014 in Hammamet, Tunisia

[12] N. Hidouri and L. Sbita, "A New DTC-SPMSM Drive Scheme for PV Pumping System, International Journal of Systems Control," vol.1.3, pp. 113-121, 2010.

[13] N. Hidouri, L. Sbita and T. Mhamdi, "An Isolated Hybrid Fuzzy Controlled-Photovoltaic Diesel-PMSG System," International Conference on Control, Engineering & Information Technology (CEIT'13), Proceedings Engineering & Technology (PET), Vol. 4, pp. 127-132, 2013.

[14] N. Hidouri, T. Mhamdi, S. Hammadi and L. Sbita, "A new hybrid photovoltaic-diesel system control scheme for an isolated load," IJRRAS, vo1. 9, issue 2, pp. 270-281, 2011.

[15] N. Hidouri, S. Hammadi and L. Sbita, "An Advanced DPC-Self Excited Induction Generator Drive Scheme for an Isolated Wind turbine Boost System," International Review on Modelling and Simulations (IREMOS), vol. 5, No. 2, pp. 913-920, 2012.

[16] M. Hedayati, "Technical Specification and Requirements of Static VAR Compensation (SVC) Protection Consist of TCR, TSC and Combined TCR/TSC," Universities Power Engineering Conference, 2004. UPEC 2004. Vol. 1, pp. 261-264, 2004.

[17] R. Mohan Mathur and R.K. Varma, "Thyristor-Based FACTS Controllers for Electrical Transmission Systems,". IEEE Press, New York (2002).